

Infrared Properties of Gold in Germanium*†

L. JOHNSON‡ AND H. LEVINSTEIN

Department of Physics, Syracuse University, Syracuse, New York

(Received September 18, 1959)

The fundamental parameters of gold in germanium have been investigated between 60–300°K by absorption, photoconductivity, and lifetime studies.

Photoconductivity measurements reveal the following capture cross sections for electrons and holes at 80°K (subscript refers to carrier being captured; superscript to charge state of gold center): $\sigma_h^- \approx 1 \times 10^{-13}$ cm², $\sigma_e^0 \approx 6 \times 10^{-14}$ cm², $\sigma_e^- \approx 10^{-17}$ cm². Lifetime studies on *n*-type samples show the existence of a 0.018-ev Coulomb barrier at singly charged sites and an indication that a thermal (phonon) mechanism is involved in the electron capture process. The lifetime also manifests itself in the noise spectrum.

The photoconductive absorption cross section at 80°K of *p*-type gold-doped germanium (0.15-ev level) is found to be 2×10^{-16} cm² at 1.8 microns. It is suggested that differences between the absorption and photoconductive spectra are due to departure from spherical symmetry of valence band contours away from $k=0$.

I. INTRODUCTION

THE first report on gold-doped germanium by Dunlap¹ proposed, on the basis of Hall effect and resistivity data, an energy level scheme consisting of two acceptor states per gold atom, at energy levels 0.20 ev below the conduction band and 0.15 ev above the valence band. Newman² extended the investigation to a study of the infrared photoconductive response of gold-doped germanium, obtaining results confirming Dunlap's model. Kaiser and Fan³ reported photoconductivity data essentially in agreement with Newman. Conductivity measurements by Morton, Hahn, and Schultz⁴ supported values of 0.18 ev above the valence band and 0.24 ev below the conduction band, and, in addition, suggested the existence of a third acceptor level at 0.05 ev above the valence band. Later investigations by Dunlap⁵ confirmed the existence of a 0.05-ev level, but identified it as a donor level. More recently, the existence of a third acceptor level has been reported,⁶ lying at 0.04 ev below the conduction band. With these modifications, Dunlap's original proposal for the behavior of gold in germanium might be described as follows: gold, with an electronic structure $5s^2 5p^6 5d^{10} 6s^1$, is assumed to enter the lattice substitutionally and to have a valence of one in germanium. The 6s electron behaves as the 0.05-ev donor, i.e., the strength of bonding of this electron to an Au–Ge pair is less than the strength of bonding of an electron to a Ge–Ge pair by 0.05 ev. The three acceptor states represent the three unsaturated Au–Ge bonds. The first acceptor state is

determined by the energy required to remove an electron from a nearby Ge–Ge bond and to place it on a neutral gold atom, or, alternatively, the minimum energy (~ 0.15 ev) required to release a hole. The second acceptor state appears only through compensation, i.e., filling the 0.15-ev lower gold levels and part of the 0.20-ev levels with electrons from added donor impurities. The upper level will then contribute *n*-type conduction by excitation of these electrons to the conduction band. Similarly, the high-lying 0.04-ev level appears when both lower acceptor levels have been compensated.

II. PREPARATION OF SAMPLES

Germanium single crystals were grown by Mr. Alfred Mac Rae, using both the Kyropolous⁷ seed-in-melt method and a technique based on the zone refining process.⁸ For most crystals, successive purifications were made, prior to doping, until *n*-type material with less than 10^{14} carriers/cm³ was obtained. Hall mobilities varied between 3000 and 3500 cm²/volt-sec.

Antimony was used when compensation of acceptor impurities was desired. Doping elements were Johnson, Matthey, and Company spectrographically standardized gold and antimony.

Crystals were first cut into slabs perpendicular to the axis of crystal growth, to maximize sample homogeneity, and then cut into samples of various sizes ranging from cubes $3 \times 3 \times 3$ mm³ to bars $2 \times 2 \times 10$ mm³ for Hall and resistivity measurements. Samples were etched in a 70% HNO₃–30% HF chemically pure etch solution and washed in doubly distilled water.

For photoconductivity measurements, ohmic contacts to *p*-type samples were made with Johnson-Matthey indium, while tin or a composition of 63% Pb–35% Sn–2% Sb low melting point alloy was used for *n*-type samples. Samples were soldered to copper blocks to provide good thermal contact, and the assembly was mounted in the cavity of a demountable metal cryostat

* Work supported by Wright Air Development Center.

† This paper is abstracted from part of a thesis by L. Johnson presented to Graduate School, Syracuse University, in partial fulfillment of the requirements for the Ph.D. degree.

‡ Now at the Bell Telephone Laboratories, Murray Hill, New Jersey.

¹ W. C. Dunlap, Jr., Phys. Rev. **91**, 1282 (1953).

² R. Newman, Phys. Rev. **94**, 278 (1954).

³ W. Kaiser and H. Y. Fan, Phys. Rev. **93**, 977 (1954).

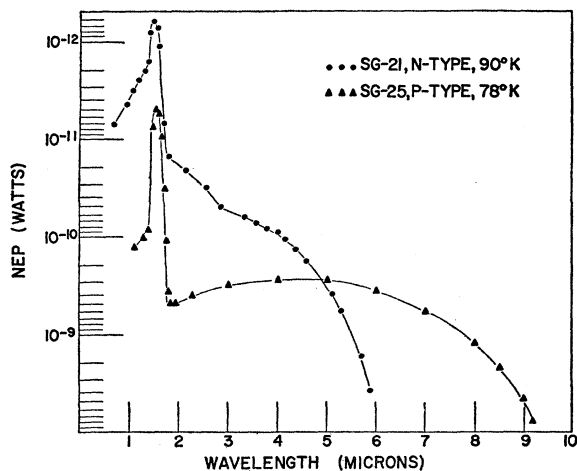
⁴ G. A. Morton, E. E. Hahn, and M. L. Schultz, *Photoconductivity Conference*, edited by R. J. Breckenridge *et al.* (John Wiley & Sons, Inc., New York, 1956), p. 556.

⁵ W. C. Dunlap, Jr., Phys. Rev. **100**, 1629 (1955).

⁶ H. H. Woodbury and W. W. Tyler, Phys. Rev. **105**, 84 (1957).

⁷ S. Kyropolous, Z. anorg. u. allgem. Chem. **154**, 308 (1926).

⁸ W. G. Pfann, J. Metals **4**, 747 (1952).

FIG. 1. Spectral sensitivity of *n*- and *p*-type Au-doped Ge.

fitted with a AgCl window. A copper cylinder served as radiation shield.

III. PHOTOCONDUCTIVE SPECTRA

A comparison of the absolute spectral sensitivity of an *n*-type sample, SG-21, and a *p*-type sample, SG-25, at 78°K, is shown in Fig. 1.⁹ The response for the *n*-type sample extends to about 6 microns; the *p*-type response to about 9 microns. Three points are of particular interest:

- (1) the structure in the intrinsic region at 1.4 microns;
- (2) higher sensitivity for the *n*-type than the *p*-type sample in the intrinsic region 0.5–1.4 microns;
- (3) an apparent superposition of spectra in the *n*-type sample in the extrinsic region 1.8–2.8 microns.

(1) The structure in the intrinsic region of a *p*-type sample, SG-37, is shown more clearly on an expanded scale in Fig. 2. Included in the graph is the absorption spectrum¹⁰ of pure germanium at 77°K. The correlation between the photoconductive and absorption spectra is clearly evident. The structure at 1.4 microns (0.88 eV) has been interpreted by Dash and Newman as arising from the onset of direct transitions.¹¹ At 77°K, the intrinsic edge for indirect transitions is seen to be at 1.72 microns (0.72 eV) from the absorption data and at 1.8 microns (0.69 eV) from the more sensitive photoconductive spectrum. Since the photoconductive response intersects the absorption spectrum at an absorption constant of 10^{-1} cm^{-1} , and since the relative intrinsic response extends more than a decade below its value at this point, the intrinsic photoconductive spectrum in this region of low absorption can be considered to be an

⁹ The scale chosen for the ordinate is Noise Equivalent Power. This is essentially the energy flux necessary to produce a signal-to-noise ratio of unity.

¹⁰ W. C. Dash and R. Newman, *Phys. Rev.* **99**, 1151 (1955).

¹¹ J. Bardeen, F. J. Blatt, and L. H. Hall, *Photoconductivity Conference*, edited by R. J. Breckenridge *et al.* (John Wiley & Sons, Inc., New York, 1956), p. 146.

extension of the absorption spectrum down to a value of $8 \times 10^{-3} \text{ cm}^{-1}$. If the impurity response is subtracted from the total response, leaving the true intrinsic response, then the absorption spectrum can be determined down to a value of $3 \times 10^{-3} \text{ cm}^{-1}$ (this is shown in Fig. 2 as the dotted extension of the intrinsic response). Extrapolating the impurity response into the true intrinsic response, the absorption coefficient for impurity photoconductivity has the value $8 \times 10^{-3} \text{ cm}^{-1}$ at 1.77 microns for sample SG-37.

(2) Regarding the greater sensitivity of *n*-type gold-doped germanium in the intrinsic region, it is seen from the absorption spectrum that energy is very highly absorbed in this region. One hole-electron pair is produced per absorbed photon in the wavelength region 1.0–1.7 microns.¹² Thus pairs are generated primarily within a small thickness near the surface where recombination is high and lifetimes short. However, some carriers will diffuse a considerable distance into the interior, if their bulk lifetimes are sufficiently long. An approximate value for the diffusion distance *L*, before recombination, may be calculated from the relation:

$$L = (D\tau)^{1/2},$$

where *D* = diffusion coefficient, τ = bulk lifetime. The diffusion coefficient is given by the Einstein relationship:

$$D/\mu = kT/e,$$

where μ is the mobility; *k* = Boltzmann's constant;

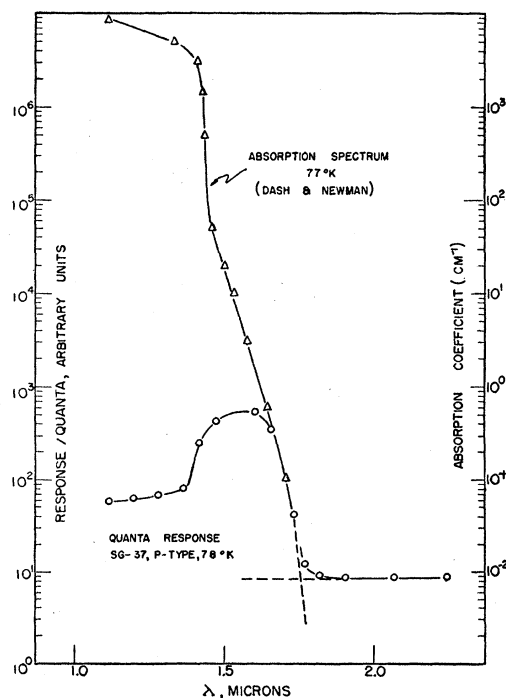


FIG. 2. Absorption and photoconductive spectra at 77°K.

¹² F. S. Goucher, *Phys. Rev.* **78**, 816 (1950).

T = absolute temperature. At 77°K, and for a mobility of 10^4 cm²/volt-sec for both electrons and holes,

$$D \approx 80 \text{ cm}^2/\text{sec.}$$

For the n -type sample, the electron lifetime $\tau_e = 150 \mu\text{sec}$ is dominant, while in the p -type sample both hole and electron lifetimes are less than 10^{-6} seconds. Hence, the diffusion distances L_n in the n -type sample and L_p in the p -type sample are:

$$\begin{aligned} L_n &\sim 1 \text{ mm,} \\ L_p &< 0.1 \text{ mm.} \end{aligned}$$

For other samples differences in bulk lifetimes leading to different diffusion lengths satisfactorily account for variations in intrinsic sensitivity of both n -type and p -type gold-doped germanium.

(3) The third feature of the photoconductive behavior, the superposition of spectra in the extrinsic region of n -type gold-doped germanium, would be expected to arise from a combination of photoionization of electrons from the valence band to the 0.20-ev gold level and from both gold levels to the conduction band. To determine which processes are dominant, a study of the dependence of time constant on wavelength was undertaken. In particular, the lifetime of an electron in the conduction band or a hole in the valence band should be dependent on whether the recombination center was a hole in the valence band, or a neutral, singly, or doubly charged gold atom.

IV. LIFETIMES AND CAPTURE CROSS SECTIONS IN p -TYPE AU-DOPED GERMANIUM

The experimental technique employed consisted of inserting a variable slit and variable speed square-wave chopper at the entrance port of a Perkin-Elmer monochromator, in the path of a beam from a tungsten lamp or globar source coming to focus on the entrance slit. The emergent monochromatic beam was focused onto the sample, the response fed through a cathode follower to a model 450 A Hewlett Packard amplifier, and the rise-decay behavior displayed on a Tektronix Type 535 Oscilloscope. For the observation of effects having a duration of several seconds, a 20 μfd condenser coupled the signal to the cathode follower, and a Tektronix Type 53-B dc amplifier replaced the Hewlett Packard amplifier. The arrangement was limited to decay times greater than 4 microseconds, the onset time for the beam. The radiation intensity was kept sufficiently low so as to assure linearity between photo-signal amplitude and radiation intensity, at least in the regions of low absorption. In this range, one would expect an exponential rise and decay for the case of a single monomolecular recombination process, with a time constant $\tau = 1/\beta N$, where β = recombination coefficient, N = density of recombination centers. It should be mentioned that only rarely did the traces fit an exponential accurately. Hence, for the purpose of discussion, the time

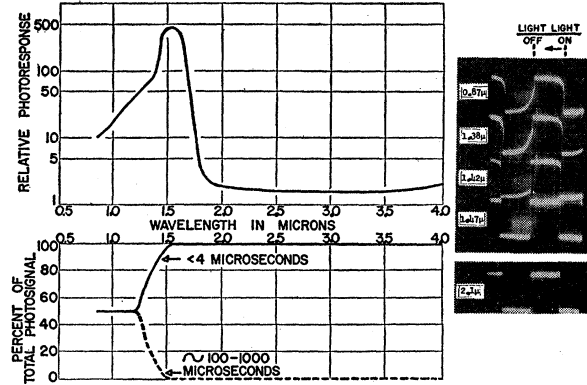


FIG. 3. Wavelength dependence of time constant for p -type Au-doped Ge. (Time base on oscilloscope tracings: 1 m sec per division; amplitude of tracings: 5 mv/div across 100 000-ohm load.)

constant for the rise will be defined as the time required to reach 63% of the final resistance value and for the decay, that required to reach 37% of the initial value.

Oscilloscope traces of the rise-decay behavior of a p -type sample as a function of wavelength are shown in Fig. 3. A summary of the dependence of time constant on wavelength is also shown in Fig. 3, with a logarithmic plot of relative spectral response superimposed to illustrate the correlation between the photoconductive and time constant spectra. Behavior in three separate wavelength regions will be distinguished:

(a) Extrinsic Region, beyond 2 Microns

In the region of impurity photoionization the lifetime is shorter than the chopper onset time. Hence τ was calculated by combining the relative spectral sensitivity curve, the measured signal from 500°K blackbody radiation, and the 80°K impurity absorption spectrum (see Sec. VI). In a simple series circuit consisting of battery, photoconductor, and load resistor, the voltage change (ΔV) appearing across the load resistor when low level illumination of appropriate wavelength falls on the sample is given by:

$$\Delta V = \frac{IR_C R_L}{R_C + R_L} \frac{G\tau}{n_0}, \quad (1)$$

where I = current, R_C = sample resistance, R_L = load resistance, n_0 = "dark" free carrier concentration, G = rate of generation of carriers per unit volume, τ = lifetime of liberated carrier.

The generation rate for blackbody radiation is given by:

$$G = N_a \int \sigma_\nu c N(\nu) d\nu, \quad (2)$$

where N_a = compensated acceptor concentration, σ_ν = absorption cross section of acceptors for photons of

frequency ν , c =velocity of photon beam in medium, $N(\nu)$ =density of photons of frequency ν .

From these two expressions we find lifetimes ranging from 2×10^{-9} to 4×10^{-7} sec. Variations of lifetimes are due to differences in density of recombination centers (negatively charged gold atoms resulting from the presence of donors). This may be seen in the expression for lifetime

$$\tau = \frac{1}{N_D \sigma_h^- v}, \quad (3)$$

where v =average thermal velocity of holes, N_D =concentration of occupied 0.15-ev gold levels (Au^- atoms), and σ_h^- =capture cross section of an Au^- impurity for a hole.

When donors are present in a p -type semiconductor (as is always the case in practice), the following expression can be derived:¹³

$$\frac{p(N_D + p)}{N - N_D - p} = \frac{N_C}{2} e^{-\Delta E/kT} = A, \quad (4)$$

where N =acceptor concentration, p =free hole concentration, $N_C = 2(2\pi m^* kT/h^2)^{3/2}$ =effective density of states in the valence band, m^* =effective mass of a hole in valence band, ΔE =acceptor activation energy (0.15 ev), A =equilibrium constant. Below 150°K, $p \ll N - N_D$; then:

$$p = [(N - N_D)/N_D] A. \quad (5)$$

N_D is computed from (5) with $N - N_D$, the uncompensated acceptor concentration, given by a Hall measurement; p is calculated from the resistivity and the mobility dependence $\mu \propto T^{-2.3}$ ($\mu = 3000$ cm²/volt-sec at 300°K); $A = 1.87 \times 10^8/\text{cm}^3$ at 80°K, using an effective mass,¹⁴ $m^* = 0.3m_0$ (m_0 =free electron mass). N_D for a variety of samples is found to cover a range 4×10^{12} to 7×10^{14} atoms/cm³. This includes samples from intentionally compensated crystals and crystals to which no donors were added.

At 80°K the kinetic theory average thermal velocity in a Maxwellian velocity distribution is $\bar{v} = (8kT/\pi m^*)^{1/2} = 10^7$ cm/sec. Inserting these values into (3) we find the capture cross section of an Au^- atom for a hole to be:

$$\sigma_h^- = 1 \times 10^{-13} \text{ cm}^2.$$

This represents the average of the cross section computed for some 50 samples, the total spread being about a factor of 2 on either side of this value.

(b) Intrinsic Region, 1.7 Microns

Referring again to Fig. 3, the wavelength interval, 1.5–1.7 microns, is in the intrinsic region of photo-

ionization, although the absorption coefficient in this range is small ($\alpha < 10 \text{ cm}^{-1}$). Hence, the intrinsic ionization and recombination processes are taking place largely in the bulk of the sample rather than at the surface. Now, the extrinsic process in p -type gold-doped germanium involves the excitation of an electron from the valence band to a 0.15-ev gold acceptor level (Fig. 4). The lifetime of the hole freed by this process before capture by singly-charged gold atoms is 10^{-9} to 10^{-7} sec, depending on N_D . In the 1.5–1.7 micron intrinsic region one might say that the recombination process involved the direct capture of an electron in the conduction band by vacant states in the valence band. But these states are few; furthermore, if such a mechanism were probable, it should be independent of sample type. Since a time constant of less than 4 microseconds does not appear in n -type behavior, one can conclude that this is not a dominant process. The intrinsic recombination process, then, for a generated hole-electron pair in p -type gold-doped germanium must involve the capture of the hole by singly charged gold atoms and the electron by neutral gold atoms, both ground states lying at the 0.15-ev gold level, and both lifetimes being less than 4 microseconds [Fig. 4(a)]. The calculation from (1) and (2) gives the value of 0.02 microsecond for a hole lifetime in this particular sample. No p -type crystals were found to have electron or hole lifetimes, in the low absorption region, large enough to permit measurement by the above technique, i.e., greater than 4 microseconds. But a simple analysis of the photosignal in this region enables one to calculate the electron lifetime in p -type material, from which one obtains σ_e^0 , the capture cross section of neutral gold atoms for electrons: $\sigma_e^0 = 6 \times 10^{-14} \text{ cm}^2$ (see Appendix).

(c) Intrinsic Region, below 1.5 Microns

Figure 3 shows that below 1.5 microns, the behavior consists of two distinctly different mechanisms, each contributing to the total signal amplitude an amount depending on wavelength. A fast component, $\tau < 4$ microseconds, is present in both rise and decay at all wavelengths. However, the fraction of the total photosignal amplitude attributed to the fast component is smaller on the decay than on the rise. This is a region of

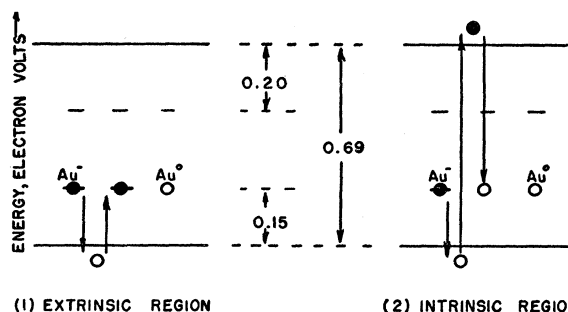


FIG. 4. Dominant electronic photoionization and recombination processes in p -type Au-doped Ge at 77°K.

¹³ See, for example, W. Shockley, *Electrons and Holes in Semiconductors* (D. Van Nostrand Company, Inc., Princeton, New Jersey, 1950), Chap. 16.

¹⁴ Dresselhaus, Kip, and Kittel, *Phys. Rev.* **92**, 827 (1953).

high absorption with all hole-electron pairs being generated in a narrow surface layer. The fast component presumably arises from the diffusion of holes and electrons into the interior of the crystal, where they are rapidly captured by gold recombination centers.

In addition, a slow component exists with a varying decay characteristic (~ 400 – 1200 microseconds) differing from a variable rise (~ 100 – 1000 microseconds). The decay is also characterized by a delay in the initial decay rate. The slow component is most likely due to trapping of carriers in various surface states. After the light is removed these carriers contribute to the signal as they are released from the traps. The delay in the initial decay rate and the smaller percentage contribution of the fast component to the total decay amplitude than to the rise supports the argument.

A brief comment should be made on the value obtained for the capture cross section of an Au^- atom for a hole ($\sigma_h^- = 1 \times 10^{-13} \text{ cm}^2$). Such an exceptionally large capture cross section for a single atom (~ 100 times an atomic dimension) might arouse some skepticism. However, suppose it is postulated that capture of a free hole by an attractive Coulomb potential occurs at that distance R_0 such that the magnitude of the potential energy of interaction $e^2/\epsilon R_0$ is equal to the kinetic energy of the free particle plus the binding energy $E_i = 0.15 \text{ ev}$:

$$(e^2/\epsilon R_0) = \frac{1}{2}mv^2 + E_i,$$

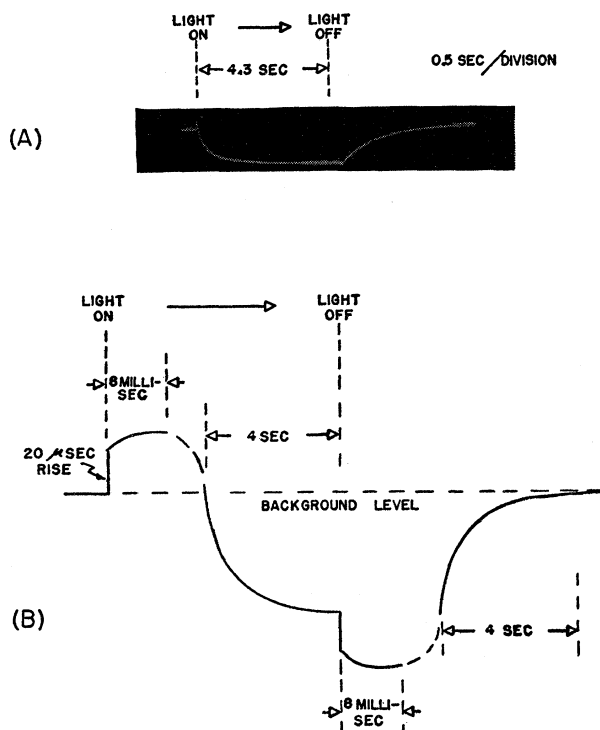


FIG. 5. Quench effect in n -type Au-doped Ge when exposed to 2-micron radiation. (a) Oscilloscope tracing. (b) Composite drawing of rise-decay behavior.

where $\epsilon = 16$ = dielectric constant. Taking the kinetic energy to be the average thermal energy $\frac{3}{2}kT$ at 80°K , we find:

$$\sigma = \pi R_0^2 \simeq 1 \times 10^{-14} \text{ cm}^2.$$

This approach yields a capture cross section a factor of 10 too small. But the study of recombination radiation has shown that the radiative process is an improbable one in Au-doped germanium, i.e., capture is most likely accompanied by absorption or emission of phonons.¹⁵ Let us suppose that capture is accompanied by emission of a phonon of energy E_p (or phonons of total energy E_p):

$$(e^2/\epsilon R_0) = \frac{1}{2}mv^2 + E_i - E_p,$$

and compute the phonon energy required to agree with the experimental value of σ_h^- . We find:

$$E_p = 0.1 \text{ ev.}$$

By coincidence, perhaps, this is the energy difference between 0.05- and 0.15-ev gold states, suggestive of an Auger-type process at the gold center (energy transfer by excitation of the atom to a higher state).

V. LIFETIME MEASUREMENTS, n -TYPE AU-DOPED GERMANIUM

A. Wavelength Dependence and Quenching

The dependence of time constant on wavelength in n -type gold-doped germanium is more complex. In addition to the expected appearance of another time constant in the superposition region, a quenching phenomenon occurs.¹⁶ Quenching will be defined as a decrease in conductivity under illumination; a typical oscilloscope trace for 2 micron radiation is shown in Fig. 5(a). Figure 5(b) is a composite drawing which illustrates the rise-decay behavior in the quench region, including both the shape of the initial response and the quench. The conductivity at first rises sharply under illumination, then decreases slowly ($\tau \sim 1 \text{ sec}$) to a value lower than before the radiation was turned on. When light is removed, the conductivity initially decreases sharply, then increases slowly to the level set by 300°K background radiation. The wavelength region of quench is shown in Fig. 6, where we define

$$\% \text{ quench} = \frac{\text{initial peak} - \text{steady state}}{\text{background level of conductivity}}.$$

The onset of quench occurs at about 2.4 microns (0.52 ev), rises sharply to a peak at 1.85 microns

¹⁵ H. Gummel and M. Lax, *Ann. Phys. (N. Y.)* 2, 28 (1957); M. Lax, *J. Phys. Chem. Solids* 8, 66 (1959).

¹⁶ Quenching effects in n -type gold-doped germanium have been investigated extensively by R. Newman, *Phys. Rev.* 94, 278 (1954). Certain unexplainable phenomena associated with quenching prevented his specifying a mechanism in detail and, in particular, one which involved gold centers. Some of the effects reported by Newman were not found in our samples, and this has led to our model for quenching which explicitly involves gold.

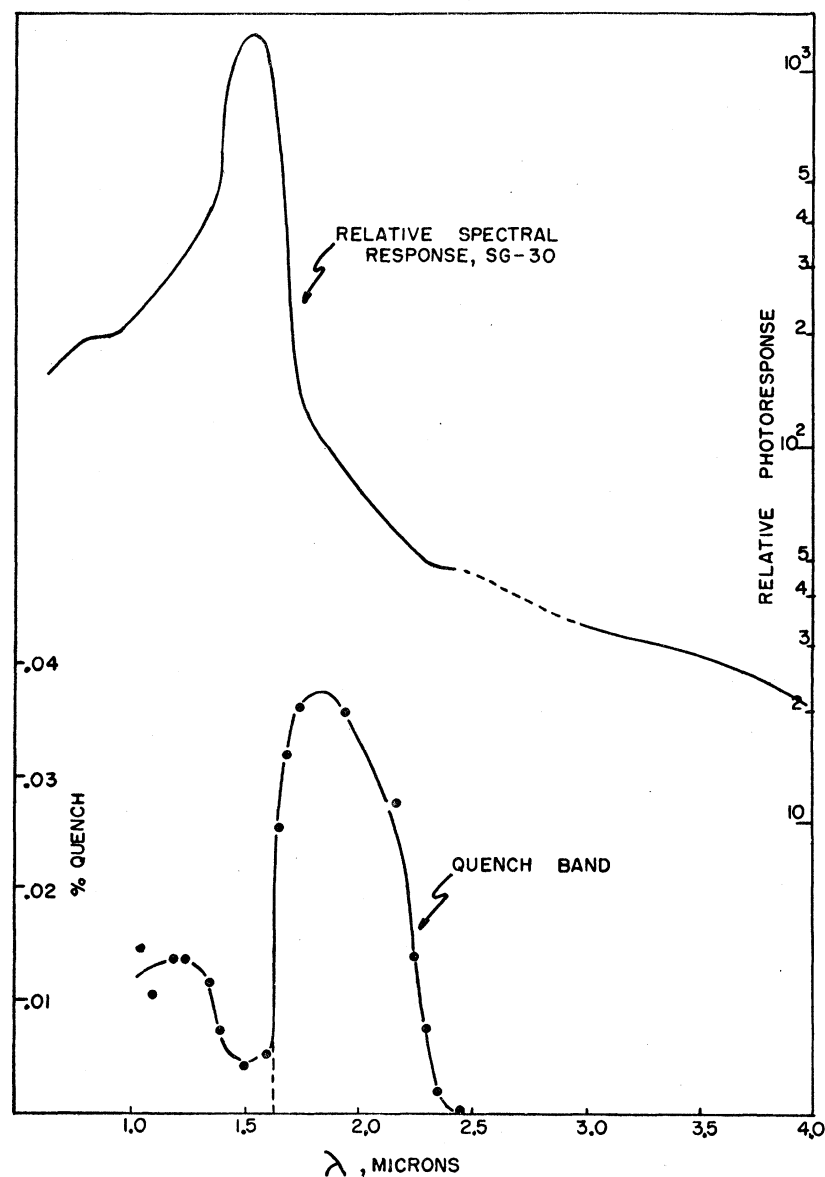


FIG. 6. Quench spectrum, *n*-type Au-doped Ge (sample SG-30).

(0.67 eV) and then decreases sharply at the intrinsic edge.

Oscilloscope traces of the rise-decay behavior as a function of wavelength for this sample are shown in Fig. 7. In the superposition region chopping speeds are such that quenching is not observed, and only the shape of the initial rise when light is turned on and decay when light is turned off is recorded. Beyond 2.4 microns, rise and decay are identical and are characterized by a time constant of about 20 microseconds. This is the region of photoionization of electrons from the upper gold level to the conduction band (0.20 eV), with recombination to singly-charged gold atoms [Fig. 8(a)]. Time constants in the region beyond 2.4 microns have been found to range from 10–1000 microseconds for different samples.

Below 2.4 microns a slow component, of the order of 10 milliseconds, contributes more and more to the total photosignal as the intrinsic peak is approached. Rise and decay traces are symmetrical down to 1.5 microns. In this region one expects to observe transitions:

- (a) from the valence band to empty states in the upper level, and
- (b) from the lower acceptor states, which are now filled with electrons, to the conduction band.

These ionization and recombination processes are shown in Fig. 8(b). Figures 6 and 7 show that the onset of the slow component occurs at the same wavelength as that for quenching. Analysis of the various recombination possibilities reveals that only the process of ionization

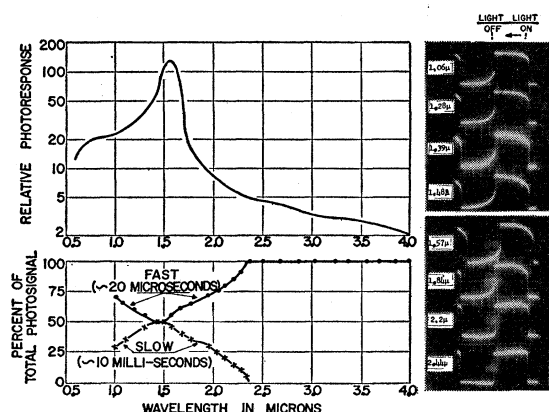


FIG. 7. Wavelength dependence of time constant before quenching for *n*-type Au-doped Ge (time base for oscilloscope tracings: 2 milliseconds per division; amplitude 2 mv/div across 1-megohm load).

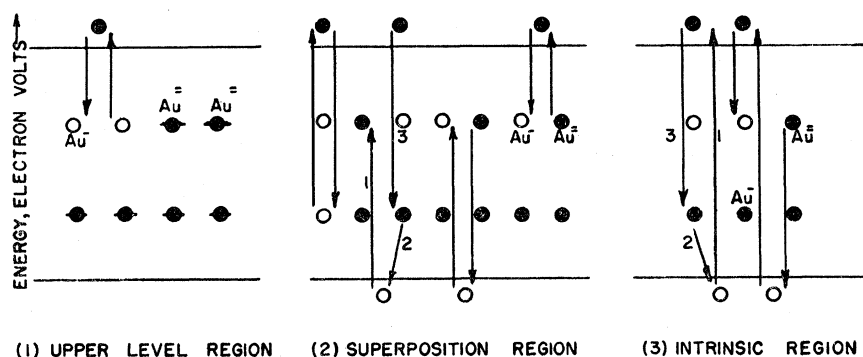
from the valence band to the upper gold level can lead to quenching. The model proposed for quenching consists of a three-step process of exciting an electron from the valence band to a vacant upper state, capture of a freed hole by an electron in the lower gold state (Au^- atom) and then recombination of a conduction band electron with the hole in the lower state (Fig. 9). The net result has been the trapping of a conduction band electron in an upper gold state (equilibrium will not be restored until this electron is reexcited to the conduction band by 300°K background radiation after light has been removed). It is to be remembered that two other processes are taking place simultaneously: excitation from both the lower and upper levels to the conduction band. From the data on *p*-type samples, hole capture by Au^- atoms is very rapid ($\sim 10^{-9}$ – 10^{-6} second). Thus, the initial spike when light is turned on is due to the rapid rate of capture of holes in lower gold states (step 2 in Fig. 9) and the rapid rate at which equilibrium with the radiation is established between the upper level and the conduction band. Thus, the two processes of hole capture by Au^- atoms and excitation from the lower level to the conduction band are creating electron vacancies in the lower gold states. If the first process were not occurring, then the latter would have a chance

to come to equilibrium with the radiation field. In other words, if there were no holes being created in the valence band to be subsequently captured by Au^- atoms, then under low-level illumination the trace pattern should be represented by two response times, characterizing excitation from and recombination to the lower and upper level respectively. Furthermore, the process involving the lower state would be expected to be much slower, since only those vacancies created by light can take part in recombination. And indeed, it can be seen from Fig. 6(b) that following the initial increase in conductivity (\sim microseconds) there is a slow increase in conductivity (\sim milliseconds) before quenching sets in. If quenching were not to follow, the time associated with this slower component would be characteristic of the rate of approach to equilibrium for the process of electron generation from the 0.15-ev state to the conduction band.

However, two "times" do not characterize the total response pattern in the "light on" stage and we must have a third time, i.e., a "quench time." This comes about as a result of the disturbance created by hole capture in the lower level. Thus, while electron excitation from and recombination to the lower and upper levels are processes which, by themselves, can come to equilibrium with the radiation field, the process from the valence band to the upper level followed by hole capture in the lower level is one which can never come to equilibrium with the radiation field. Hence, the background level of conductivity must shift to achieve a balance, i.e., conduction band electrons will be required to fill the vacancies created by hole capture in the lower gold states. The net result will be a reduction or a "quenching" of the "dark carrier" electron concentration in the conduction band during the "light on" cycle.

From the difference in conductivities before and after quenching the density of electrons quenched can be determined ($4 \times 10^6 \text{ cm}^{-3}$ for Fig. 5(a)). This also reveals the density of centers rendered capable of quenching by the incident radiation. With the observed quench time of 0.5 sec, and a thermal velocity of about 10^7 cm/sec , one finds the capture cross section of these centers to be $5 \times 10^{-14} \text{ cm}^2$. In the Appendix it is shown that this agrees with the capture cross section of neutral gold

FIG. 8. Dominant electronic photoionization and recombination processes in *n*-type Au-doped Ge at 77°K .



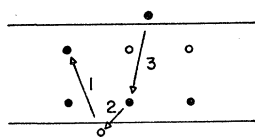


FIG. 9. Model of the quenching process in *n*-type Au-doped Ge.

atoms for electrons, as expected according to the quenching model.

When the 2 micron radiation is removed, return to equilibrium occurs in about 1.5 sec [Fig. 5(a)]. The rate equation for equilibrium between background radiation and electrons in the 0.2-ev level shows the generation rate per doubly charged gold atom to be 0.4 sec^{-1} for the background level on the sample of Fig. 5(a). This means a transition time of 2.5 sec for electrons trapped in the 0.2-ev level (net result of quenching), in reasonable agreement with the observed 1.5 sec.

B. Temperature Dependence of Lifetime and Capture Cross Section in *n*-Type Gold-Doped Germanium

The behavior of time constant with temperature in *n*-type Au-doped germanium has been observed over the temperature range 60–120°K. Measurements were confined to an investigation of the upper gold level, by recording oscilloscope traces of the decay for low intensity 3 micron radiation. The results on four samples are plotted in Fig. 10 in the form $\log \tau$ vs $1/T$. Two regions of behavior of the form $\tau = \tau_0 e^{\Delta E/kT}$ are clearly indicated: a rapidly changing function of temperature above 100°K, and a more slowly varying function below 100°K. The processes involved are more clearly seen when the resistance of a typical sample is plotted in the

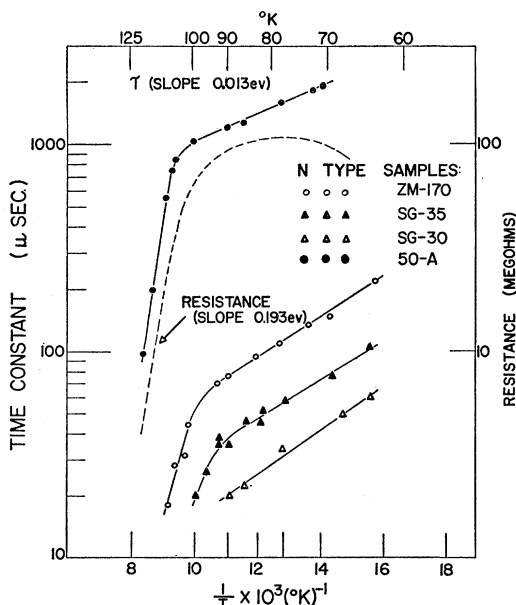


FIG. 10. The variation of time constant (solid lines) and resistance (dotted line) with temperature for various *n*-type Au-doped Ge samples.

same manner as the time constant (Fig. 10). It can be seen that above 100°K the time constant approaches the slope of the resistance curve, indicating that a thermal mechanism governs the behavior of the time constant. Below about 90°K the dark carrier concentration is invariant with temperature, due to the level of background radiation; the resistance decreases due to an increase in mobility. However, the time constant continues to increase with decreasing temperature but with a new value of ΔE ($\langle \Delta E \rangle = 0.018 \text{ ev}$). In this region the time constant should be given by:

$$\tau = \frac{1}{(N - N_D + n_0) \sigma_e^- v}, \quad (6)$$

where $N - N_D$ = density of vacant upper gold states at absolute zero (recombination centers), σ_e^- = capture cross section of Au^- atoms for an electron, v = average thermal velocity. Since N , N_D , and n_0 are invariant and τ is only weakly temperature-dependent, the capture cross section must be of the form:

$$\sigma_e^- = \sigma_0 e^{-\Delta E/kT}. \quad (7)$$

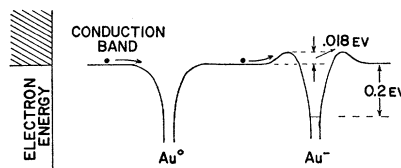


FIG. 11. Model showing the repulsive Coulomb screen in the vicinity of a negatively charged Au ion.

To get a physical picture of such behavior it will be recalled that the vacant upper gold recombination states are all singly charged gold atoms due to filling of the lower 0.15-ev level. Hence, while a neutral gold atom acts like an unscreened potential well for the capture of electrons, a singly charged Au atom possesses a repulsive Coulomb screen for electrons which raises the lip of the well by about 0.018 ev (Fig. 11).

At 90°K we find from (6) that $\sigma_e^- \sim 10^{-17} \text{ cm}^2$. It seems unreasonable to say that by converting a neutral gold atom to a singly charged gold atom the cross section for electron capture is reduced from $6 \times 10^{-14} \text{ cm}^2$ to $\sim 10^{-17} \text{ cm}^2$, a reduction by a factor ~ 6000 . However, since the effectiveness of the Coulomb screen depends on the thermal energies of the free carriers it may be possible that at 90°K its influence is very significant. On the other hand, at thermal energies sufficiently high that $kT \gg \Delta E$, one would expect that the Coulomb screen will have lost its effectiveness and the cross section for electron capture should approach that of a neutral gold atom:

$$\sigma_e^- = \sigma_e^0 e^{-\Delta E/kT},$$

where σ_e^0 = electron capture cross section of Au^0 atoms, $\Delta E = 0.018 \text{ ev}$. However, at 90°K, we find:

$$\sigma_e^- \approx \frac{1}{10} \sigma_e^0 \approx 6 \times 10^{-15} \text{ cm}^2.$$

Hence, the Coulomb screen cannot account for the large reduction in capture cross section which is indicated. But we can see from Fig. 10 that a more drastic mechanism governs the lifetime at higher temperatures, for the lifetime departs from a 0.018-ev slope at about 100°K. We note from Fig. 10 that this is also the temperature at which the resistance starts to approach its characteristic 0.20-ev slope. Yet this is not a region where n_0 is sufficiently large to reduce the lifetime in Eq. (6) (n_0 is still much smaller than $N - N_D$). Hence, the variation in lifetime must again reflect the temperature dependence of the capture cross section, and a thermal (or at least a strongly temperature-dependent) process must be involved in the actual act of capture itself¹⁵ (in distinction to the role that temperature plays in determining the density of recombination centers). The time constant appears to have the same slope as the resistance. This is not completely certain since the time constant becomes very short within a small temperature range. But it appears that above 100°K the process involved in thermal ionization, i.e., interaction between gold atoms and lattice vibrations (phonons), is also the mechanism by which electrons are captured at Au⁻ sites. Below 100°K capture is influenced by Coulomb repulsion at the center.

With this interpretation let us consider again the significance of the constant σ_0 in (7). With $\sigma_0 \sim 10^{-17}$ cm² at 90°K, we find $\sigma_0 \sim 10^{-16}$ cm², i.e., of the order of an atomic dimension. The form of (7) states that σ_0 is the value of electron capture cross section of Au⁻ atoms at temperatures sufficiently high that $kT \gg \Delta E$, i.e., when the Coulomb screen is no longer effective. We observed that this would make the Au⁻ atom appear neutral to the incoming electron, but we find that the capture cross section thus obtained ($\sim 10^{-16}$ cm²) is much smaller than the value found for the electron capture cross section of Au⁰ atoms in *p*-type germanium. It is believed that no discrepancy exists because there is a fundamental difference between these two situations: depth of the ground state. *n*-Type capture proceeds to the 0.20-ev state; *p*-type, to the deeper 0.15-ev state. Tighter binding implies components of higher momentum in the bound state wave function. When it is remembered that phonons have high momenta but low energy, we see that the probability for transfer of energy between electrons and lattice vibrations may be governed primarily by the selection rule on exchange of momentum. The wider the spread in the distribution of momenta in the ground state wave function the greater the probability that high-momentum phonons may participate in capture, and the larger the capture cross section.

As a final point of interest, we may use the value $\Delta E = 0.018$ ev at a singly charged gold atom to determine the magnitude of the scattering potential at any multiply charged impurity site. The work of Tyler and

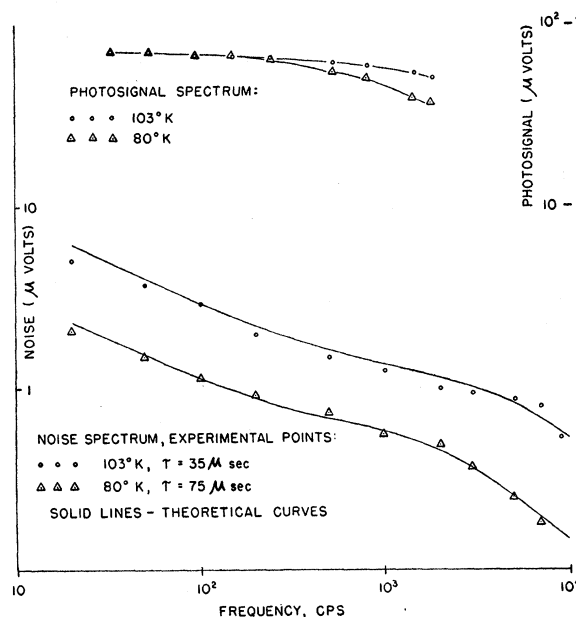


FIG. 12. Noise and photosignal spectra of a characteristic *n*-type Au-doped Ge sample.

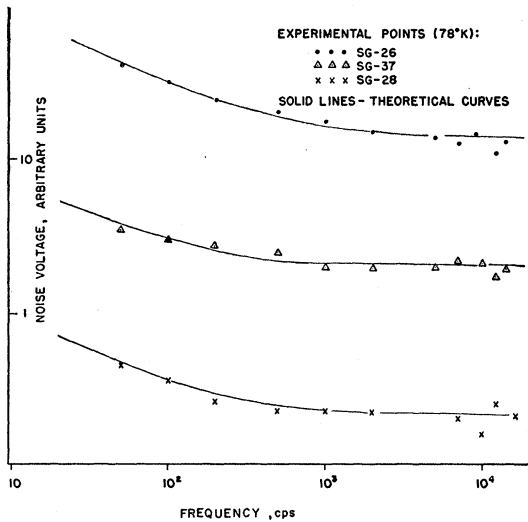
Woodbury¹⁷ on mobility in germanium with multiply charged impurities has shown that the scattering cross section follows a Z^2 dependence for $Z = 1, 2$, or 3 (Z is the charge on the impurity center). Hence, the magnitude of the screening potential at a doubly charged gold atom would be about 0.07 ev, and 0.16 ev at a triply charged site.

C. Noise Spectra

In evaluating the photosensitivity of *n*- and *p*-type gold-doped germanium it was observed that while photoconductive signals from *n*-type specimens were invariably greater than from *p*-type, noise levels were also greater. Signal levels are higher primarily because of a longer lifetime before recombination at gold centers, so one asks if there is a factor contributing to noise which arises from fluctuations in the generation-recombination rates at gold centers. If so, then it should have a characteristic time identical with the photoconductive decay time.

In the previous section it was shown that the lifetime in *n*-type Au-doped germanium depends rather strongly on temperature. Hence, a noise component associated with gold levels should manifest itself by a shift with temperature in the same manner as the lifetime. The noise voltage spectra of a representative *n*-type sample at two temperatures are shown in Fig. 12. The photosignal characteristics are also included for comparison. The noise spectra can be represented by two com-

¹⁷ W. W. Tyler and H. H. Woodbury, Phys. Rev. **102**, 647 (1956); H. H. Woodbury and W. W. Tyler, Phys. Rev. **105**, 84 (1957).

FIG. 13. Noise spectrum of a typical *p*-type Au-doped Ge sample.

ponents such that:

$$V \propto \left(\frac{K_1^2}{f} + \frac{K_2^2}{1 + \omega^2 \tau^2} \right)^{\frac{1}{2}}, \quad (8)$$

where $f = \omega/2\pi$ = measuring frequency, and K_1 and K_2 are parameters which are independent of frequency. The first term is the familiar $1/f$ contribution to noise power; the second represents the frequency dependence of a generation-recombination (*g-r*) component having characteristic time τ .

The solid lines in the noise spectra of Fig. 12 were obtained by inserting the photoconductive time constant (measured by decay to 3-micron radiation) into (8) and weighting the parameters K_1 , K_2 to obtain the best fit to the experimental points. It is seen that the choice of photoconductive lifetime for the characteristic time in the *g-r* component gives a good fit to the data. Furthermore, the required characteristic time follows the same variation with temperature as the lifetime, clearly identifying this component with generation-recombination fluctuations for the 0.20-ev gold level.

The parameter K_2 has been shown by van Vliet¹⁸ to be given by:

$$K_2^2 = (4I^2/n_0)\tau,$$

where I = dc current, and n_0 = total number of free carriers in sample. This may be compared with experiment by computing the amplitude of the *g-r* noise component from the measured total noise voltage and the weighted curve which best fits the data (making appropriate corrections for bandwidth and load resistor). K_2 as determined from van Vliet's expression is found to be about a factor of 2-3 larger than the experimental value.

Noise spectra for *p*-type samples are shown in Fig. 13.

¹⁸ K. M. van Vliet, Proc. Inst. Radio Engrs. 46, 1004 (1958).

Since photoconductive lifetimes are in the range 10^{-9} to 10^{-6} sec, the knee of a *g-r* component would occur in the 0.1-100 Mc region ($\omega\tau \sim 1$). The flat portion, therefore, represents the *g-r* component in the range $\omega\tau \ll 1$.

VI. OPTICAL ABSORPTION IN *p*-TYPE AU-DOPED GERMANIUM

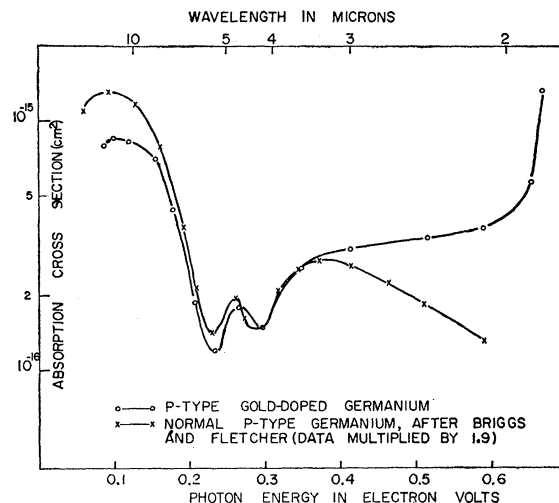
A. Absorption Measurements

The experimental arrangement for transmission measurements is as follows: radiation dispersed by a spectrometer equipped with CaF_2 or NaCl prism is collected and focused onto the sample; the transmitted energy is then collected and monitored by a thermocouple. Both continuous recording and sample in-sample out techniques were used. For measurements at liquid nitrogen temperature, samples were mounted in a Dewar equipped with AgCl windows. Window corrections were made by comparing room temperature sample transmissions with and without windows. This was found necessary due to somewhat nonuniform transmission of the AgCl .

The expression for the energy transmitted by a plate with parallel faces at normal incidence, taking into account multiple internal reflections is given by:¹⁹

$$T = \frac{I}{I_0} = \frac{(1-R)^2 e^{-\alpha X}}{1 - R^2 e^{-2\alpha X}},$$

where I_0 and I are the incident and transmitted intensities, respectively; R is the reflectivity,²⁰ α = absorption coefficient (cm^{-1}), and X = sample thickness (cm). Over a range for which $\alpha X \ll 1$, $T = [(1-R)/(1+R)] = 0.47$. Thin specimens of pure germanium were found

FIG. 14. Absorption cross section of Au-doped Ge and normal *p*-type Ge at 295°K.

¹⁹ R. B. Barnes and M. Czerny, Phys. Rev. 38, 338 (1931); H. Y. Fan and M. Becker, *Semiconducting Materials* (Butterworth's Scientific Publications, London, 1951), p. 132.

²⁰ Over the range investigated, $R = [(n-1)/(n+1)]^2$ where n = index of refraction = 4.

to exhibit about 47% transmission in regions of low absorption (3–11 microns), but thick samples frequently did not. This occurred when faces were not perfectly parallel following polishing operations. The necessity of using a small area thermocouple resulted in a portion of the internally reflected energy not being focused onto the thermocouple, the effect being magnified in thick specimens. To eliminate this difficulty, samples were oriented a few degrees from normal incidence so that internally reflected energy was not recorded by the thermocouple. Under these conditions the transmission is given by:

$$T = (1-R)^2 e^{-\alpha X},$$

where $\alpha X \ll 1$, transmissions of 41–42% were observed for pure specimens. A value of 41% should be obtained for a reflectivity $R=0.36$.

Transmission measurements were made on several samples, differing in thickness and gold concentration. Results from measurements on a 1-cm thick *p*-type Au-doped germanium sample at 80°K and 295°K are shown in Figs. 14 and 15.

B. Discussion

The sample contains about 2×10^{15} gold acceptor atoms per cm^3 . At 295°K these holes are free and give rise to the well-known absorption associated with valence band interband transitions.²¹ A comparison of the absorption spectra of Au-doped germanium and "normal" *p*-type germanium²² at 295°K is shown in Fig. 14. Lattice absorption has been subtracted,²³ and the absorption coefficient α has been divided by the free hole concentration to obtain a cross section. The magnitude of the absorption cross section is in closer agreement with the data of Kaiser, Collins, and Fan while the shape more nearly resembles that of Briggs and Fletcher. Hence, to illustrate the difference in absorption between

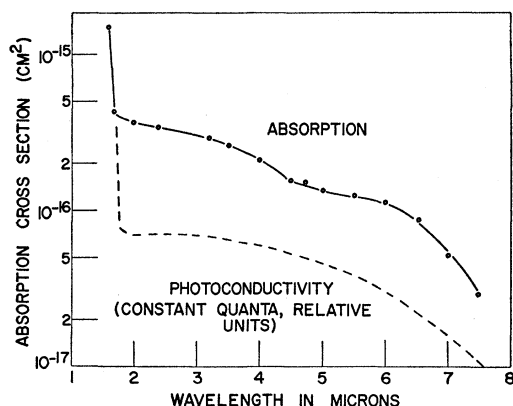


Fig. 15. Absorption cross section of *p*-type Au-doped Ge at 85°K.

²¹ H. B. Briggs and R. C. Fletcher, Phys. Rev. **87**, 1130 (1952); **91**, 1342 (1953); W. Kaiser, R. J. Collins, and H. Y. Fan, Phys. Rev. **91**, 1380 (1953).

²² "Normal" refers to group III acceptors.

²³ W. F. Simeral, thesis, Michigan, 1953 (unpublished).

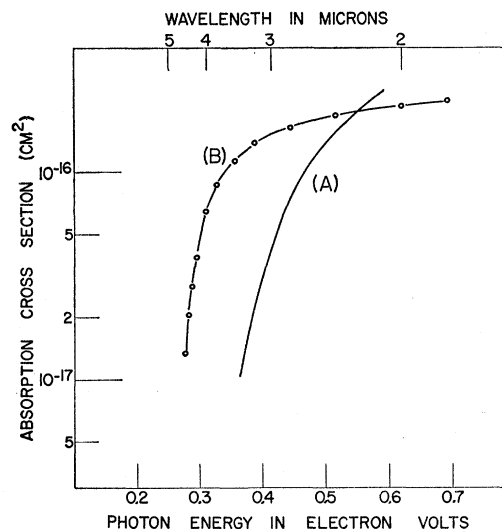


Fig. 16. (A) Absorption in excess of normal free hole absorption at 295°K. (B) Excess absorption at 85°K.

Au-doped and normal *p*-type germanium at 295°K, the data of Briggs and Fletcher was used, multiplied by a factor of 1.9. The spectra are seen to be quite similar except in the region above 0.4 ev. Interband transitions account for absorption bands at 0.26 ev, 0.4 ev, and the broad band below 0.2 ev. However, Au-doped germanium exhibits an additional absorption at 295°K which overlaps the band at 0.4 ev and extends to the main absorption edge at 0.65 ev.

At 85°K the sample exhibits photoconductivity to about 9 microns. Most of the holes arising from the 2×10^{15} gold atoms per cm^3 are trapped on gold acceptors 0.15 ev from the valence band, leaving only $\sim 10^{10}$ free holes per cm^3 in the valence band. Thus interband transitions will not be observed. The absorption spectrum at 85°K is shown in Fig. 15. The absorption coefficient α has been divided by the gold concentration N to obtain an absorption cross section σ per gold atom ($\alpha = N\sigma$).

There exist, then, two aspects of the absorption spectra which require closer examination: the absorption at 85°K not observed in photoconductivity, and the absorption above 0.35 ev at 295°K in excess of the absorption characteristic of normal *p*-type germanium. These two features are illustrated more clearly when the absorption predominating in photoconductivity has been subtracted from the 85°K spectrum (Fig. 15). The results are shown in Fig. 16. It is seen that the bands of excess absorption at 85°K and 295°K differ both in threshold and sharpness at the knee. The absorption at 295°K is believed to arise from hole transitions to the heavy mass band from the gold acceptor state 0.20 ev from the conduction band. At this temperature holes are liberated from the 0.15-ev acceptor states and undergo the interband transitions of normal *p*-type germanium. Holes are still bound to an acceptor state above the

middle of the forbidden band, however, and may undergo transitions to the valence band. Taking the minimum separation between valence and conduction bands at 0.62 eV at 300°K,¹⁰ the threshold for these transitions should lie at 0.42 eV. This is considered to be in fair agreement with curve (A) of Fig. 16 in view of the fact that this absorption overlaps the 0.4-eV interband absorption. Electron transitions from the 0.15-eV levels to the conduction band are also possible at 295°K, beginning at 0.47 eV, and this may tend to obscure any plateau region in curve (A) of Fig. 16. In this connection, it should be pointed out that the comparison with the 300°K data of Kaiser, Collins, and Fan²¹ indicated more clearly the presence of two overlapping bands.

At 85°K it is believed that the mechanism suggested for the excess absorption at 295°K does not apply (electron transitions from valence band to 0.20-eV level). Three reasons are given for this. First, at 85°K the lower 0.15-eV acceptors are now empty (of electrons), and the 0.20-eV state probably does not exist under this condition; i.e., the upper state appears only when the lower state is occupied.²⁴ Second, if transitions between valence band and 0.20-eV states were possible, it would be difficult to account for a shift in threshold to lower energy (curve B, Fig. 16). At this temperature holes are bound to 0.15-eV acceptors and intuitively one would expect this to depress the 0.20-eV state rather than shift it closer to the valence band. Thirdly, an increase in the intrinsic energy gap with decrease in temperature would also work in the opposite direction.²⁵ Furthermore, the process should contribute to photoconductivity, although the lifetime may be too short to be significant. Thus the explanation proposed is that the excess absorption at 85°K arises from vertical hole transitions from 0.15-eV acceptors to valence band states which are far removed from the center of the Brillouin zone at $k=0$. That such is possible is indicated by the following: a hole bound to a deep acceptor implies a greater spread in k space than a hole bound to a shallow group III acceptor. For example, localizing a hole on a 0.15-eV gold acceptor to a radius appropriate to an absorption cross section of 2×10^{-16} cm² (Fig. 14)²⁶ requires momentum components in the bound hole wave function extending to $\sim 10^8$ cm⁻¹ in k space, i.e., all the way to the zone boundary. The excess absorption at 85°K would represent then the shape of a valence band energy surface (probably the heavy mass band) between points well removed from $k=0$ and the zone boundary. The

transitions are shown schematically in Fig. 17. They are in contrast to those allowed for indium acceptors, where bound holes possess wave vector components extending only to $\sim 10^7$ cm⁻¹. If complete knowledge of the bound hole wave function were known (say from spin resonance experiments) then, in principle, the valence band contour could be determined. According to this interpretation there should be a correlation between the low-temperature photoconductive and absorption spectra of Au acceptors and the spectra for other deep-level acceptor impurities. Photoconductivity of deep levels has been studied extensively²⁷ but absorption has been measured only for Cu (0.04 eV),³ Zn (0.03 eV),²⁸ and Ni.²⁷ Cu exhibits an absorption excess somewhat similar to Au, but Ni apparently does not. Thus one is not yet certain whether the excess absorption at low temperature in p -type Au-doped germanium is a reflection of the

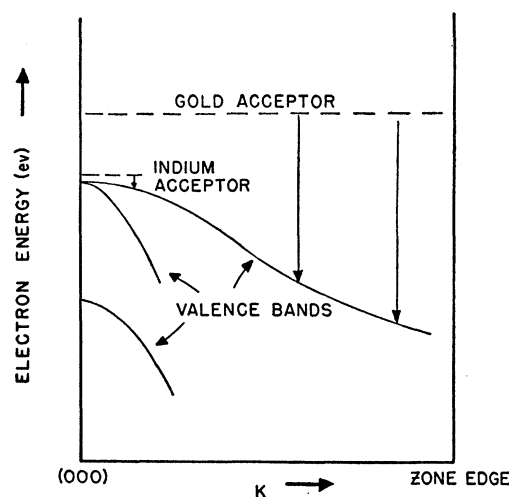


FIG. 17. Bound hole absorption in Ge.

contour of a valence band energy surface or represents behavior specifically identified with Au impurity.

VII. APPENDIX

The following method was used to determine σ_e^0 , the capture cross section of neutral gold atoms for electrons. As mentioned previously, when hole-electron pairs are generated in p -type Au-doped germanium, holes are captured by Au^- atoms and electrons by Au^0 atoms. In the vicinity of the intrinsic absorption threshold the total photoresponse (S) is given by:

$$S \propto \alpha_i(\tau_e^0 + \tau_h^-) + \alpha\tau_h^-,$$

where α_i = intrinsic absorption coefficient, α = impurity

²⁴ The situation is as follows: a neutral gold atom presents three acceptor states which are triply degenerate at 0.15 eV from the valence band. A doubly degenerate 0.20-eV state appears when an electron occupies one of the 0.15-eV levels. Similarly, the high 0.04-eV level appears when a 0.20-eV state is occupied.

²⁵ Incidentally, it has been pointed out that as the energy gap increases the 0.15-eV level remains fixed relative to the valence band: W. Kaiser and H. Y. Fan, *Phys. Rev.* **93**, 977 (1954).

²⁶ Obtained from Fig. 15 by extrapolating to the intrinsic threshold at 1.8μ that portion of the absorption spectrum observed in photoconductivity. This value was also used to calculate time constants from photoconductivity data (see Sec. IV).

²⁷ See, for example, R. Newman and W. W. Tyler in *Solid State Physics*, edited by F. Seitz and D. Turnbull (Academic Press, Inc., New York, 1959), Vol. 9, p. 49.

²⁸ Burstein, Picus, and Sclar, *Photoconductivity Conference*, edited by R. J. Breckenridge *et al.* (John Wiley & Sons, Inc., New York, 1956), p. 253.

absorption coefficient, τ_e^0 , τ_h^- are electron and hole lifetimes.

Suppose we have a sample in which $\tau_e^0 \ll \tau_h^-$, which implies $N - N_D \gg N_D$, where $N - N_D$ = the concentration of uncompensated (neutral) gold atoms. If we now compare the intrinsic photoresponse curve of this sample with one for which $N - N_D/N_D < 1$, we can determine τ_e^0 (see Fig. 18); that is:

$$\frac{S_1}{S_2} = \frac{(\alpha_i + \alpha_1)\tau_{h1} + \alpha_i\tau_{e1}}{(\alpha_i + \alpha_2)\tau_{h2}},$$

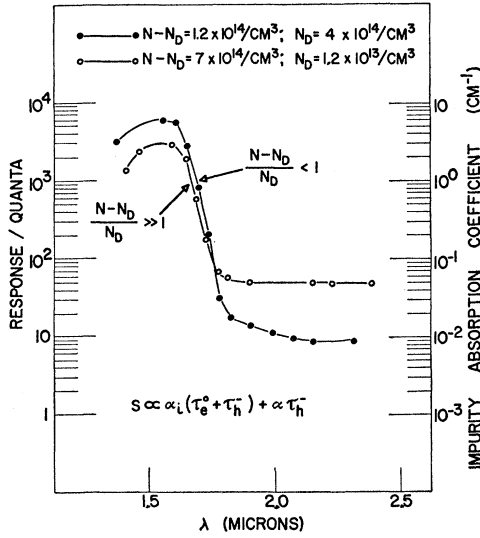


FIG. 18. Influence of electron lifetime on intrinsic response in *p*-type Au-doped Ge.

where α_1 and α_2 are impurity absorption coefficients of samples 1 and 2. For sample 2, $\tau_{e2}^0 \ll \tau_{h2}^-$.

TABLE I. Estimated capture cross sections in Au-doped Ge.

$\sigma_e^0 \approx 6 \times 10^{-14} \text{ cm}^2$	Electron capture by Au^0
$\sigma_e^- \sim 10^{-17} \text{ cm}^2, 90^\circ\text{K}$	Electron capture by Au^-
$\sigma_h^- \approx 1 \times 10^{-13} \text{ cm}^2$	Hole capture by Au^-
$\sigma_h^{--} > 10^{-13} \text{ cm}^2$	Hole capture by Au^{--}

Using τ_h values calculated from (1) and (2), and the observed ratio S_1/S_2 (on the low absorption side of the threshold), we find $\tau_{e1}^0 = 1.1 \times 10^{-8}$ sec for the sample in which $(N - N_D)/N_D < 1$. The electron capture cross section of Au^0 atoms is found to be:

$$\sigma_e^0 = \frac{1}{\tau_e^0 v (N - N_D)} \approx 6 \times 10^{-14} \text{ cm}^2,$$

where v , the average thermal velocity at 80°K is given by²⁹:

$$v = \left(\frac{8}{\pi}\right)^{\frac{1}{2}} \left(\frac{kT}{m_e^*}\right)^{\frac{1}{2}} = 1.4 \times 10^7 \text{ cm/sec}.$$

Using this cross section, we find $\tau_{e2}^0 = 0.2 \times 10^{-8}$ sec in the sample for which $(N - N_D)/N_D \gg 1$, compared with the calculated hole lifetime $\tau_{h2}^- = 15 \times 10^{-8}$ sec. Hence, for this sample, the condition $\tau_e^0 \ll \tau_h^-$ is fulfilled.

We find, then, that the capture cross section of a singly-charged gold atom for a hole is about a factor of 2 larger than the capture cross section of a neutral gold atom for an electron. Electron capture by singly charged atoms has been discussed in Sec. V(B). A table summarizing the estimates of capture cross sections in Au-doped germanium is presented in Table I.

²⁹ The electron effective mass was taken to be $m_e^* = 0.16m$ [R. N. Dexter, H. J. Zeiger, and B. Lax, Phys. Rev. **104**, 637 (1956)].

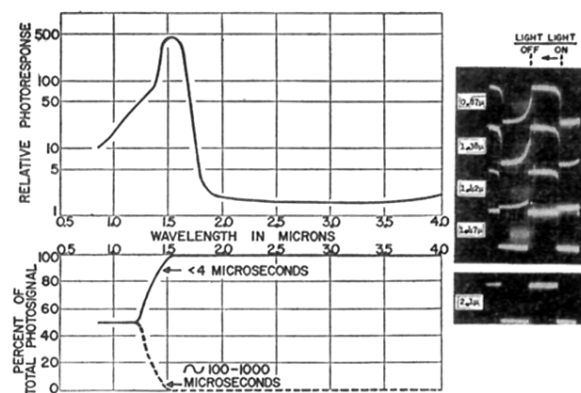


FIG. 3. Wavelength dependence of time constant for *p*-type Au-doped Ge. (Time base on oscilloscope tracings: 1 m sec per division; amplitude of tracings: 5 mv/div across 100 000-ohm load.)

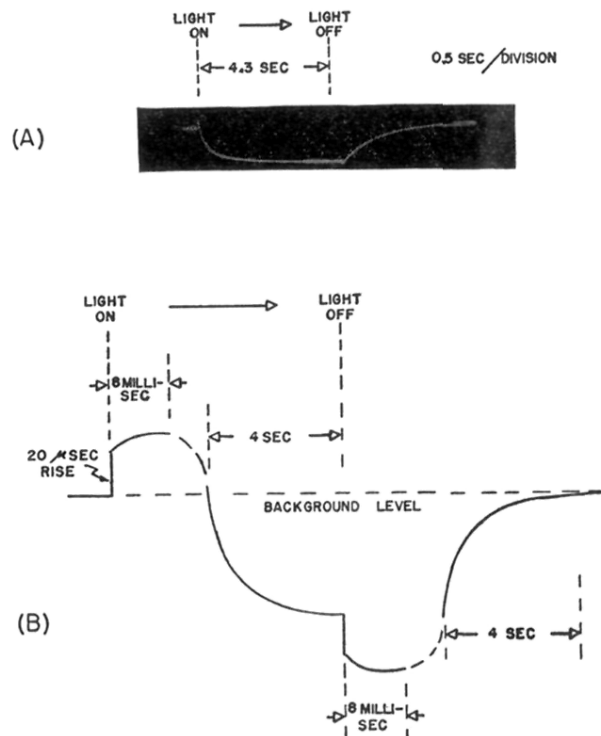


FIG. 5. Quench effect in *n*-type Au-doped Ge when exposed to 2-micron radiation. (a) Oscilloscope tracing. (b) Composite drawing of rise-decay behavior.

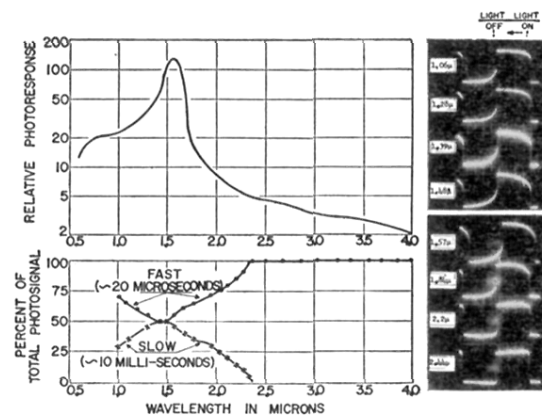


FIG. 7. Wavelength dependence of time constant before quenching for *n*-type Au-doped Ge (time base for oscilloscope tracings: 2 milliseconds per division; amplitude 2 mv/div across 1-megohm load).